KECK Geology Consortium
Learning Science Through Research
Published by the Keck Geology Consortium
Short Contributions
Keck Geology Consortium
Volume 34
May 2022
doi: 10.18277/AKRSG.2022.34.01

GEOCHEMICAL PROPERTIES OF SEEPAGE-FILTRATION AND FRACTURE SPRINGS IN WISCONSIN

ZEB PAGE, Oberlin College
REBECCA A. VANDERLEEST, Oberlin College

INTRODUCTION

Young Mountains: The Patagonian Andes

Mountains are modified over time via exhumation, erosion, and climate. Archives of past orogenic modification are recorded in the adjacent foreland basin. Provenance studies of the foreland basin examine these archives to recognize where sediment is being derived and what the origin reveals about past tectonic and magmatic activity. The Magallanes-Austral Basin, located at the southern tip of South America (Fig. 1), provides an excellent example of continuous stratigraphic section (e.g., Biddle et al., 1986; Romans et al., 2010; Daniels et al., 2018; Fosdick et al., 2020) from which provenance studies can be conducted to study past tectonic and magmatic activity. Further, this basin underwent several tectonic changes including episodes of ridge subduction (Ramos and Kay, 1992; Ramos, 2005), thrust belt advancement (Fosdick et al., 2011), and opening of oceanic passageways (Eagles and Jokat, 2014), which may be recorded in the sediment archives.

Detrital zircon ages have proven diagnostic when determining sediment sources for the southern Patagonian Andes (Fig. 2) (e.g., Schwartz et al., 2016; Leonard et al., 2020; Fosdick et al., 2020). Currently, Cenozoic-based provenance studies using modal sandstone analysis, clast counts, and detrital

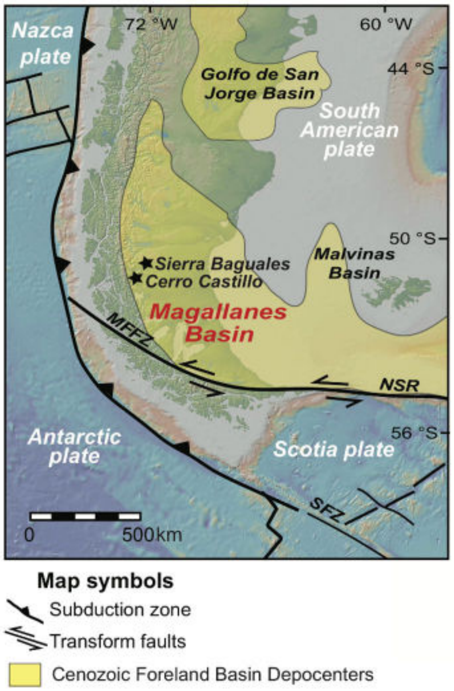

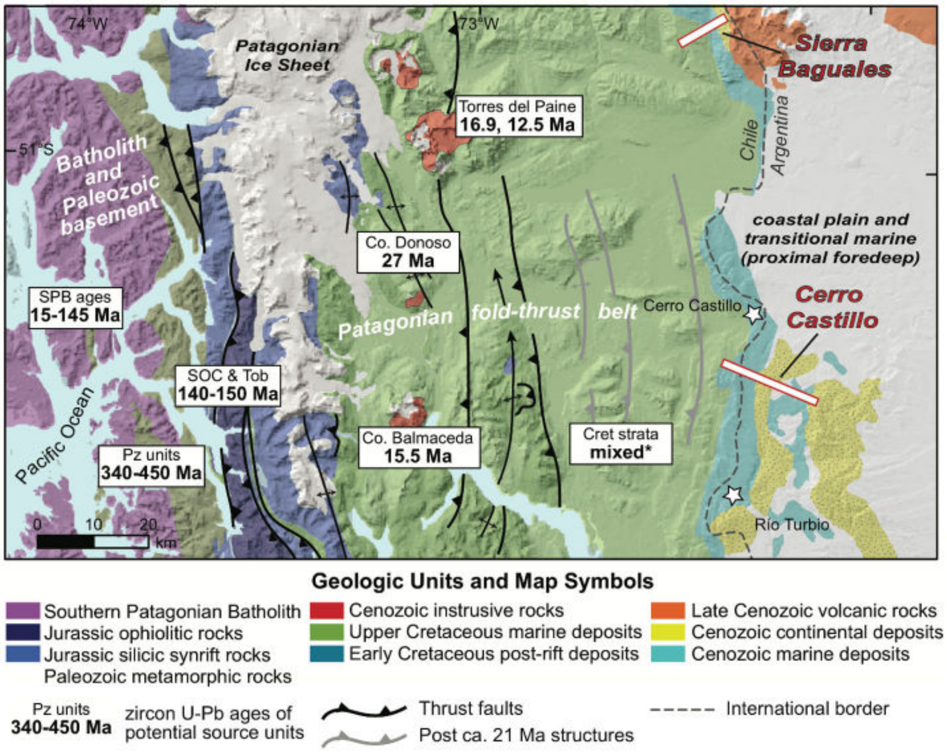

Figure 1 (Left). Tectonic setting of the Magallanes-Austral Basin.

Figure 2 (Right). Geologic map of the study area in the Patagonian Andes. Modified from Fosdick et al. (2020).

zircon ages reveal that Oligocene-Miocene fluvial sediment is dominantly sourced from the volcanic arc despite increased fold and thrust belt activity during this time in the Cerro Castillo area (Leonard et al., 2020; VanderLeest et al., 2020). Comprehensive detrital zircon ages from Cenozoic stratigraphy within Cerro Castillo reveal loss of Paleozoic and Jurassic sources throughout the Cenozoic due to Paleogene orogenesis and rise of Cretaceous sources due to fold and thrust belt activity (Fosdick et al., 2020). North of Cerro Castillo in Sierra Baguales, comprehensive provenance analysis has not been conducted. Further, the stratigraphy of the Sierra Baguales displays differences in grain size and fossil content (Ugalde et al., 2018) when compared to Cerro Castillo, and basin subsidence histories reveal slight differences in patterns of tectonic uplift (VanderLeest, 2020). These differences could signal changes in basin geometry which may reflect tectonic and magmatic differences within the Patagonian Andes between these study areas. A provenance study that captures how Cenozoic tectonics has influenced Sierra Baguales and Cerro Castillo areas would provide a more holistic view of the Ultima Esperanza region.

In 2017, detrital zircon U-Pb ages, modal sandstone and clast counts were completed for the Sierra Baguales and Cerro Castillo study areas. A total of 10 detrital zircon samples were collected from the Paleogene to Miocene section at Sierra Baguales and 10 detrital zircon samples collected from Paleogene to Miocene sections at Cerro Castillo and Cancha Carrera. Along with a total of 40 sandstone petrographic thin section samples and clast counts between the two study areas. We will analyze the detrital zircon age populations and geochemistry along with the modal sandstone and clast count datasets to determine origin of the sediment and unravel tectonic and magmatic phases within the Ultima Esperanza region of the Patagonian Andes to understand differences between these two study areas.

Ancient Mountains: The Adirondacks

The Adirondack Mountains of New York are a fragment of the exposed core of a massive, worldwide mountain-building event known as the Grenville Orogeny. The geology of the Adirondacks is notoriously complex and records multiple episodes of subduction, collision and igneous intrusion from 1.3 to 1.05 Ga (e.g., Heumann et al., 2006). Sedimentary basins formed along the margin of the Laurentian continent, including detrital zircons similar to those being studied in the "Young Mountains" project (e.g., Chiarenzelli et al., 2015), which were heated to the point of partial melting during the collisional episodes, growing new zircon that dates the metamorphism (e.g., Heumann et al., 2006; Bickford et al., 2008). In addition to growing new zircon, metamorphic minerals such as biotite and garnet formed, the chemistry of which can be used to determine the conditions of metamorphism.

The study of metamorphism in the Adirondacks has been ongoing for more than a century. The first widespread application of a modern thermodynamic approach to the study of metamorphism established high temperatures (>700˚C) across the Adirondack Highlands, with the highest temperatures found in the center of the region (Bohlen et al., 1985). More recent work focused on metamorphosed igneous rocks has established peak temperatures of up to 850˚C (Spear and Markussen, 1997). Oxygen isotope studies in the Adirondacks have likewise confirmed high regional temperatures (e.g., Peck and Valley, 2004; Quinn et al., 2016), as well as the sedimentary origin of the partially-melted rocks known as migmatites (Lancaster et al., 2008). Recent work on a small number of these partially-melted metasediments has also resulted in extremely high-temperature estimates (Storm and Spear, 2005; 2009).

Approaches to extracting temperatures and pressures from metamorphic rocks have evolved with changing technologies, and the previous paragraph cites studies using a variety of techniques. A fairly recent development in metamorphic petrology has been the use of internally calibrated X-ray composition maps to generate clouds of P-T (Pressure-Temperature) data to better evaluate the information preserved in the chemistry of zoned minerals. This approach is typically applied to quantify X-ray maps generated using Wavelength Dispersive Spectrometry. We applied this technique (with the free software package XMap Tools, Lanari et al., 2014) using Energy Dispersive Spectrometry (EDS) on predominantly un-zoned minerals from the Adirondack Highlands.

We simultaneously contribute to the P-T dataset that can be used to reconstruct the geometry of this ancient mountain range, and evaluate the use of quantitative EDS mapping for this purpose.

RESEARCH AND RESULTS

This research involved eight rising sophomore students, a rising senior peer mentor, and two faculty from Oberlin College. Students worked in two groups on their research projects. Together we had daily check-in meetings and split time collecting data on the SEM at Oberlin College for the respective projects.

STUDENT PROJECTS

Young Mountains

Sediment Provenance of the Magallanes-Austral Basin ~ 51° S Using Kernel Density Estimates from Detrital Zircon U-Pb Ages and Sandstone Composition to Analyze Tectonics and Erosional Activity

SOFIA T. BARTH, Union College; **EMILY I. BENGSTON**, Oberlin College; **AMELIA S. G. BRONFMAN**, Oberlin College; **SARAH E. BROWN**, Scripps College

We used the Scanning Electron Microscope (SEM) at Oberlin College to evaluate tectonic provenance of sandstones. Polished sandstone thin sections were carbon coated and placed in the SEM to produce Backscatter Electron (BSE) images and Energy-dispersive X-ray Spectroscopy (EDS) maps for petrographic point counting (Fig. 3). We conducted point counts using these maps and images. Point counts were complete after a total of 400 counts. We plotted the results on ternary diagrams after Dickinson and Susek (1979) in R (R Core Team, 2020).

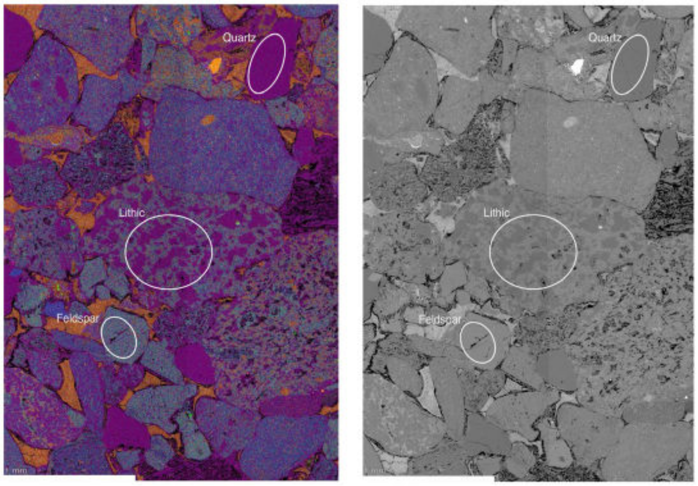

Figure 3. Left: Portion of Energy-dispersive X-ray Spectroscopy (EDS) image of thin section sample 15LDC-02 from the Cerro Dorotea formation at Cerro Castillo. We overlaid grids while counting to provide clear boundaries when point counting (not shown in figure). Elements are color coded to help identify minerals. Magenta-Si; Cyan-Na; Organge-Fe and Mg; Green-Ca; Blue-K; Yellow-Al. Right: Portion of backscatter electron image (BSE) of thin section sample 15LDC02 from the Cerro Dorotea formation at Cerro Castillo. Image includes quartz, lithic, feldspar, and calcite grains. Distinguishing textures aided in the process of identifying minerals.

Detrital zircon U-Pb ages were compiled from VanderLeest et al. (2018); Leonard et al. (2020); Fosdick et al. (2020); and Fosdick et al. (2015). We generated and analyzed KDEs and bar graphs in detritalPy (Sharman et al., 2018). This team explored how sediment provenance, including detrital zircon U-Pb ages and petrographic point counts, reflects tectonic influence over time using two study sites along strike within the Magallanes-Austral retroarc foreland basin. The Magallanes-Austral retroarc foreland basin has undergone tectonic changes due to its location inboard of the Chilean trench and Southern Patagonian Andes.

The team examined Paleocene to Miocene formations at two study sites, Sierra Baguales and Cerro Castillo (Fig. 4). From west to east, the Jurassic to Miocene Patagonian Batholith and Paleozoic metamorphic basement complexes, the Jurassic hinterland fold-and-thrust belt, and the Cretaceous fold-and-thrust belt contributed sediment to these formations (Fig. 2).

The team quantified sediment provenance using KDEs (Fig. 5; Sharman et al., 2018) and ternary diagrams after Dickinson and Suscek (1979) (Fig. 6). They discovered that pronounced zircon U-Pb age clusters from Sierra Baguales include 25-0 Ma, 40-25 Ma, 65-40 Ma, 136-80 Ma, and 175-136 Ma. Pronounced zircon U-Pb age clusters from Cerro Castillo include: 25-0 Ma, 40-24 Ma, 65-40 Ma, 80-65 Ma, 136-80 Ma, and 175-136 Ma. The KDE shows younger zircon ages upsection with the appearance of 65-40 Ma, 40-25 Ma, and 25-0 Ma in the Lower Río Turbio Formation. A decrease in 420-250 Ma and 175-136 Ma age peaks occurs upsection at both study sites. Ternary diagrams

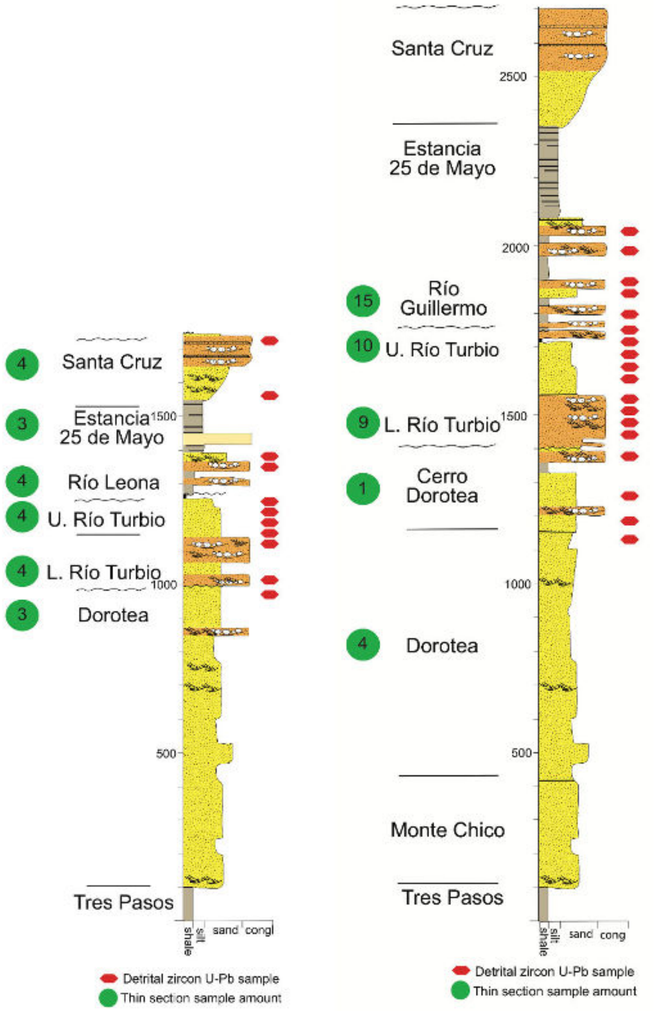

Figure 4. Left: Sierra Baguales lithostratigraphy after Fosdick et al. (2015). Right: Cerro Castillo lithostratigraphy after Fosdick et al. (2020).

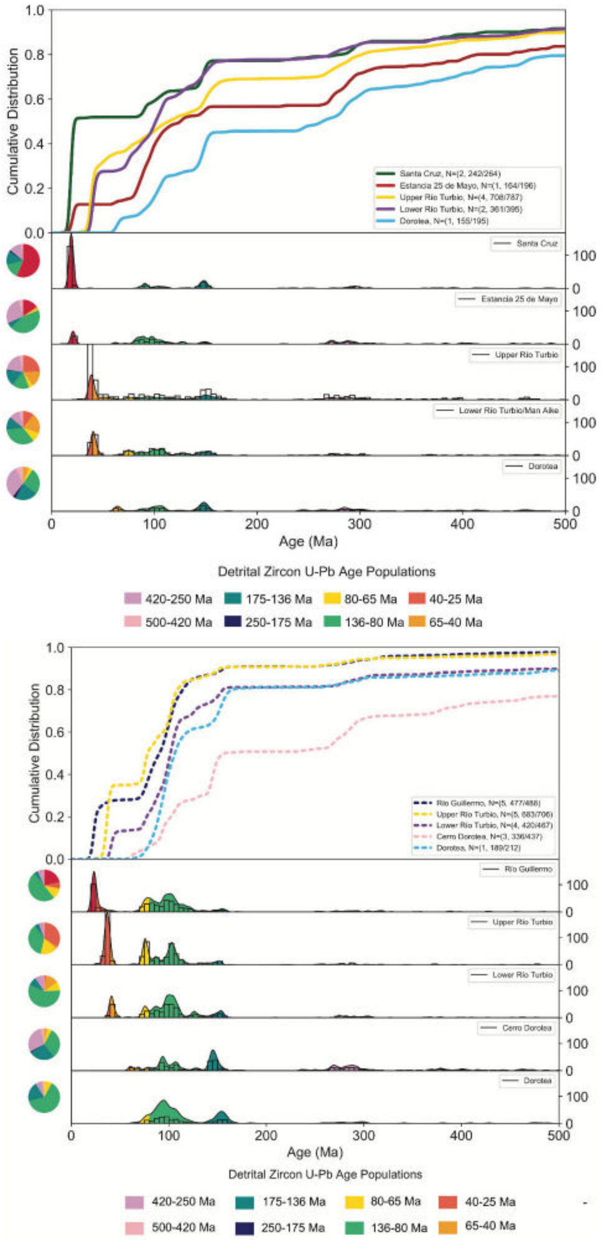

Figure 5. Left: Kernel Density Estimates (KDEs) graph of detrital zircon U-Pb data from Sierra Baguales. Detrital zircon dataset compiled from Fosdick et al. (2015) and VanderLeest et al. (2018). Right: Kernel Density Estimates (KDEs) graph of detrital zircon U-Pb data from Cerro Castillo. Detrital zircon dataset compiled from VanderLeest et al. (2018); Fosdick et al (2020); Leonard et al. (2020). KDEs generated in detritalPy (Sharman et al., 2018).

with data from both study sites show that Paleocene to mid-Eocene formations (Dorotea, Cerro Dorotea, Lower Río Turbio formations) tend to be more quartz-rich and lithic-poor than the upper Oligocene to mid-Miocene formations (Río Leona, Río Guillermo, Estancia 25 de Mayo, Santa Cruz formations).

Sediment provenance reveals that Paleocene units contain more quartz and higher proportions of zircons aged 420-250 Ma. Therefore, we suggest this sediment originated from the East Andean Metamorphic Complex, Metasedimentary Basement Complex and Patagonian Batholith. Ternary diagrams indicate Paleocene formations have a primarily mixed and dissected arc provenance consistent with the interpretation that the Patagonian Batholith was exposed during the Paleocene to mid Eocene due to erosion of the volcanic cap and/or less volcanic activity. Differences in sandstone composition and concentration of zircon age populations indicate a significant tectonic event occurred between the Paleocene units and Eocene-Miocene units. This change in provenance aligns well with the passage of the Aluk-Farallon slab window and that could be the reason for the zircon age population and sandstone composition changes. Differences in proportion of Permian, Jurassic, and Cretaceous aged zircon

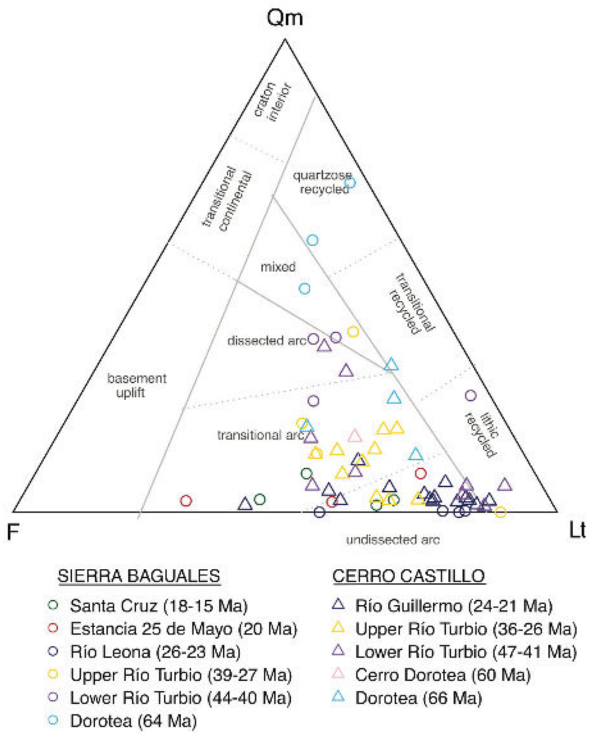

Figure 6. QmFLt ternary diagram showing tectonic provenance for Sierra Baguales and Cerro Castillo in the Magallanes-Austral Basin after Dickinson and Suczek (1979). Qm-monocrystalline quartz; F-feldspar; Lt-total lithics.

between Cerro Castillo and Sierra Baguales reveal the fold and thrust belt was more active to the south than to the north. These observations signal that hinterland orogenic growth may have been more prominent at Sierra Baguales than at Cerro Castillo.

Ancient Mountains

Survey of Adirondack Metamorphic Temperatures Using Quantitative EDS Mapping

ELISE BOUCHER, Pitzer College; **MATTEA HORNE**, Peer Mentor, Pomona College; **JOSIPHINE LISSET**, Oberlin College; **CONNER MINKOWITZ**, Franklin & Marshall College; **BEN ROCHE**, Colorado College

During the summer of 2021, the Ancient Mountains team prepared polished rock chips for EDS mapping from three classic Adirondack localities with differing lithologies. The samples studied were lecosome and melanosome from migmatitic gneiss from Treadway Mountain (08ADK-01; Heumann et al., 2006; Lancaster et al, 2008) and a coronitic olivine metagabbro (08ADK-04) at the southern margin of the Marcy Anorthosite (Johnson and Essene, 1982).

Samples were carbon coated and long term (6-18 hour duration) EDS maps were collected guided by Back-Scattered Electron (BSE) imaging using a TescanVega 3 electron microscope and Oxford XMax80 large area Silicon Drift Detector. After analysis, ~15 spot analyses were collected per mineral within the 500-1000 μm field of view. Internal virtual standards were used. Careful attention was paid to a consistent working distance and samples were well-polished and flat. EDS maps were processed in XMapTools (Lanari et al., 2014), using the drift correction to compensate for variable detector sensitivity across the field of view. Temperature estimates were made using calibrations of cation exchange thermometers built into the XMapTools software.

Thermometry results from the two samples were consistent with existing estimates using conventional methods. Application of the Ti in biotite thermometer of Henry (2003) to the Treadway Mountain migmatite sample shown in Figure 7 yields 748±18˚C. The uncertainty in this result is due to the minor variability in Ti in the biotite pixels of Fig. 7. Garnet-biotite thermometry based on X-ray maps of Figure 7 results in a much lower temperature of 651±19˚C. The low reported uncertainty indicates homogeneous composition across the pixels in the maps, and the lower temperature is expected from retrograde diffusion of Fe and Mg between garnet and biotite in contact in a granulite-facies sample.

The metagabbro sample 08ADK-04 preserves variable textures at the thin section scale from multi-phase coronas of metamorphic minerals surrounding relict igneous olivine, no more equant textures as reported by Johnson and Essene (1992) consisting of garnet, clinopyroxene, and hornblende in a plagioclase matrix (Fig. 8). Garnet-hornblende (Grt-Hbl) (Ravna, 2000a) and Garnet-clinopyroxene (Grt-CPX) exchange thermometry applied to the corresponding pixels in Figure 8 result in identical temperatures 712±44˚C (Grt-Hbl) and 712 ±35˚C (Grt-CPX). The 712˚C result is consistent with previous thermometry of these rocks (e.g., Bohlen et al., 1985); however, the increased uncertainty when compared with the previous sample suggests more heterogeneity in the map pixels, although this could be due to true sample heterogeneity or errors in the EDS map.

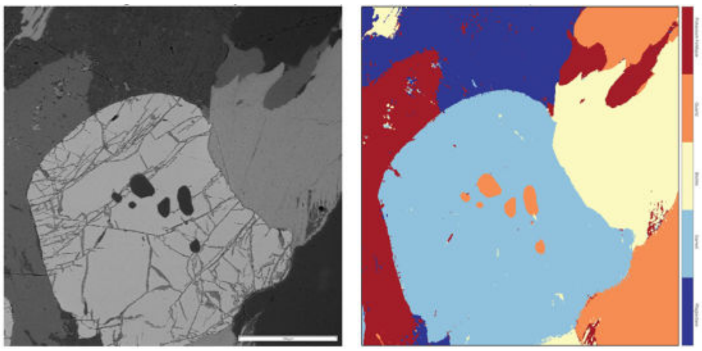

Figure 7. Left. Back-Scattered Electron (BSE) image of migmatite leucosome sample 08ADK-01 with a central garnet surrounded by potassium and plagioclase feldspars, biotite, and quartz. Right. Phase-map of the same image showing different minerals classified from X-ray maps.

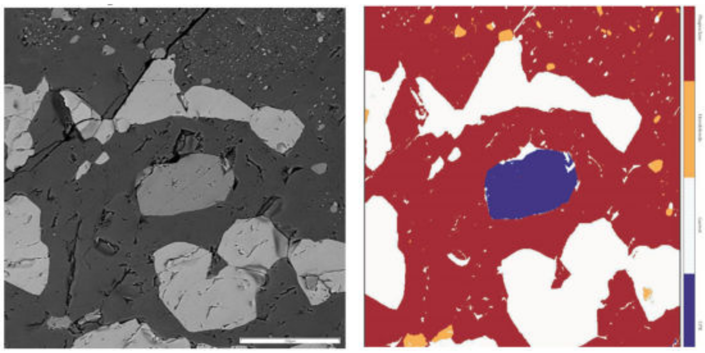

Figure 8. Left: BSE image of metagabbro 08ADK-04 with equant textures. Right: Phase map of the same field of view: garnet, plagioclase, clinopyroxene, and hornblende are present.

In order to better evaluate the precision and accuracy of this approach, we analyzed garnets from both samples using WDS point analyses by electron microprobe at the University of Michigan. The results of this comparison are presented in Figure 9. Although at first inspection, there appears to be significant scatter in the mapped compositions, these are primarily due to a small number of map pixels occurring in or along cracks or boundaries between phases. When all pixels are averaged from the full map, garnet compositions differ by less than 5% between WDS point analysis and the EDS mapping approach we used.

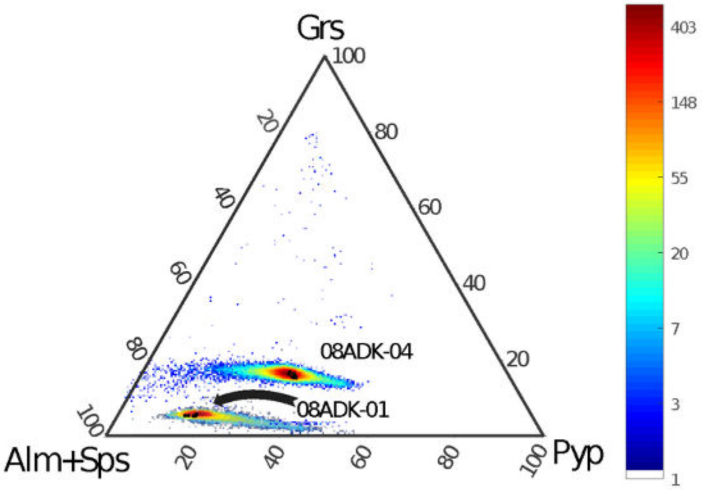

Figure 9. Ternary diagram of the composition of garnets in Adirondack migmatite (08ADK-01) and metagabbro (08ADK-04). Black points are WDS point analyses, colored points are pixels from Figs. 7 and 8 classified as garnet, the color scale is in number of pixels at a given composition. Average garnet compositions differ by less than 5% between techniques. (Grs – Grossular, Alm – Almandine, Sps – Spessartine, Pyp – Pyrope).

Thermobarometry based on quantified X-ray maps offers a new and exciting direction for metamorphic petrology. Our results suggest that careful attention to sample geometry and long counting times allow for this approach to be used with SEM-EDS. Furthermore, the use of calibrated EDS maps offers a powerful teaching tool for both mineralogical and petrological concepts such as solid solution and thermobarometry, as well as more general skills such as multi-spectral imaging, data processing, and analysis.

ACKNOWLEDGEMENTS

This research is supported by the Keck Geology Consortium and the National Science Foundation under Grant EAR-1659322. The purchase of the SEM-EDS system used in this work was supported by NSF Grant EAR-1626271. Owen Neill is gratefully acknowledged for assistance with microprobe analyses. Additional funding for this project was generously provided by the Oberlin College Department of Geosciences.

REFERENCES

Young Mountains

Biddle, K.T., Uliana, M.A., Mitchum, R.M., Fitzgerald, M.G., Wright, R.C., 1986, The stratigraphic and structural evolution of the central and eastern Magallanes Basin, southern South America. In: In: Allen, P.A., Homewood, P. (Eds.), Foreland Basins 8. Blackwell Publishing Ltd, Oxford, UK, pp. 41–61. https://doi.org/10.1002/ 9781444303810.

Fosdick, J.C., Grove, M., Graham, S.A., Hourigan, J.K., Lovera, O., Romans, B.W., 2015, Detrital thermochronologic record of foreland burial heating, sedimentary provenance, and orogenesis in Patagonia: Basin Res. 27, 546–572, https://doi.org/10. 1111/bre.12088.

Daniels, B.G., Auchter, N.C., Hubbard, S., Romans, B.W., Matthews, W.A., Stright, L., 2018, Timing of deep-water slope-evolution constrained by large-n detrital and volcanic ash zircon geochronology, Cretaceous Magallanes Basin, Chile: Geol. Soc. Am. Bull 130, 438–454.

Dickinson, W.R., and Suczek, C.A., 1979, Plate tectonics and sandstone compositions: Am. Assoc. Petrol. Geol. Bull. 63, 2164-2182.

Fosdick, J.C., VanderLeest, R.A., Bostelmann T., J.E., Leonard, J.S., Ugalde, R., Oyarzún, and Griffin, M., 2020, Revised timing of Cenozoic Atlantic incursions and changing hinterland sediment sources during southern Patagonian orogenesis: Lithosphere.

Leonard, J.S., Fosdick, J.C., VanderLeest, R.A., 2020, Dynamics of coupled surface and tectonic evolution of a retroarc orogenic wedge as revealed by sedimentary provenance: Front. Earth Sci. 7, 1–20. https://doi.org/10.3389/feart.2019.00353.

R Core Team, 2020, R: A language and environment for statistical computing. R Foundation for Statistical Computing, Vienna, Austria. URL https://www.R-project.org/

Ramos, V.A., Kay, S.M., 1992, Southern Patagonian plateau basalts and deformation: Backarc testimony of ridge collisions: Tectonophysics 205, 261–282.

Ramos, V.A., 2005, Seismic ridge subduction and topography: Foreland deformation in the Patagonian Andes: Tectonophysics 399, 73-86.

Romans, B.W., Fildani, A., Graham, S.A., Hubbard, S.M., Covault, J.A., 2010, Importance of predecessor basin history on the sedimentary fill or a retroarc foreland basin: Provenance analysis of the Cretaceous Magallanes basin, Chile (50-52 °S): Basin Res. 22, 640–658. https://doi.org/10.1111/j.1365-2117.2009.00443.x.

Schwartz, T.M., Fosdick, J.C., Graham, S.A., 2016, Using detrital zircon U-Pb ages to calculate Late Cretaceous sedimentation rates in the Magallanes-Austral basin, Patagonia: Basin Res. 29, 725–746. https://doi.org/10.1111/bre.12198.

Ugalde, R., Bostelmann, E., Fosdick, J., Alarcón, M., Oyarzún, J.L., 2018, Lithostratigraphy of the Cenozoic sedimentary series of Sierra Baguales, Magallanes, Chile: Actas digitales XV Congreso Geológico Chileno, Concepción, Chile.

VanderLeest, R.A., 2020, Detrital geothermochronology, geochemistry, and subsidence analysis of tectonics and sedimentation in the Magallanes-Austral Basin, Patagonian Andes [PhD Dissertation], 276 p.

VanderLeest, R.A., Fosdick, J.C., Leonard, J.S., Morgan, L.E., 2020, Detrital record of the late Oligocene - early Miocene mafic volcanic arc in the southern Patagonian Andes (~51°S) from single-clast geochronology and trace element geochemistry: Journal of Geodynamics 138, doi: 10.1016/j.jog.2020.101751.

Ancient Mountains

Bickford, M.E., Mclelland, J.M., Selleck, B.W., Hill, B.M., and Heumann, M.J., 2008, Timing of anatexis in the eastern Adirondack Highlands: Implications for tectonic evolution during ca. 1050 Ma Ottawan orogenesis: Bulletin of the Geological Society of America v. 120, p, 950.

Bohlen, S., Valley, J.W., and Essene, E.J., 1985, Metamorphism in the Adirondacks. I. Petrology, Pressure and Temperature: Journal of Petrology

Chiarenzelli, J., Kratzmann, D., Selleck, B.W., and Delorraine, W., 2015, Age and provenance of Grenville supergroup rocks, Trans-Adirondack Basin, constrained by detrital zircons: Geology v. 43, p, 183–186.

Heumann, M.J., Bickford, M.E., Hill, B.M., Mclelland, J.M., Selleck, B.W., and Jercinovic, M.J., 2006, Timing of anatexis in metapelites from the Adirondack lowlands and southern highlands: A manifestation of the Shawinigan orogeny and subsequent anorthosite-mangerite-charnockite-granite magmatism: Bulletin of the Geological Society of America v. 118, p, 1283.

Johnson, C.A., and Essene, E.J., 1982. The formation of garnet in olivine-bearing metagabbros from the Adirondacks. Contributions to Mineralogy and Petrology 81, 240–251.

Lanari, P., Vidal, O., De Andrade, V., Dubacq, B., Lewin, E., Grosch, E.G., and Schwartz, S., 2014, XMapTools: A MATLAB©-based program for electron microprobe X-ray image processing and geothermobarometry: Computers & Geosciences v. 62, p, 227–240.

Lancaster, P.J., Fu, B., Page, F.Z., Kita, N.T., Bickford, M.E., Hill, B.M., Mclelland, J.M., and Valley, J.W., 2008, Genesis of metapelitic migmatites in the Adirondack Mountains, New York: Journal of Metamorphic Geology v. 27, p, 41–54.

Peck, W.H., and Valley, J.W., 2004, Quartz-garnet isotope thermometry in the southern Adirondack Highlands (Grenville Province, New York): Journal of Metamorphic Geology v. 22, p, 763–773.

Quinn, R.J., Kitajima, K., Nakashima, D., Spicuzza, M.J., and Valley, J.W., 2016, Oxygen isotope thermometry using quartz inclusions in garnet: Journal of Metamorphic Geology v. 35, p, 231–252.

Ravna, E.K., 2000a. Distribution of Fe2+ and Mg between coexisting garnet and hornblende in synthetic and natural systems: an empirical calibration of the garnet-hornblende Fe-Mg geothermometer. Lithos 53, 265–277.

Ravna, E.K., 2000b. The garnet-clinopyroxene Fe2+-Mg geothermometer: an updated calibration. Journal of Metamorphic Geology 18, 211–219.

Spear, F.S., and Markussen, J.C., 1997, Mineral zoning, PTXM phase relations, and metamorphic evolution of some Adirondack granulites, New York: Journal of Petrology v. 38, p, 757.

Storm, L.C., and Spear, F.S., 2005, Pressure, temperature and cooling rates of granulite facies migmatitic pelites from the southern Adirondack Highlands, New York: Journal of Metamorphic Geology v. 23, p, 107–130.

Storm, L.C., and Spear, F.S., 2009, Application of the titanium-in-quartz thermometer to pelitic migmatites from the Adirondack Highlands, New York: Journal of Metamorphic Geology v. 27, p, 479–494.